

SOLAR SYSTEM CONSTRAINTS ON THE YUKAWA POTENTIAL IN f(R) GRAVITY

Romy Hanang Setya Budhi*

Departemen Fisika, Fakultas Matematika dan Ilmu Pengetahuan Alam, Universitas Gadjah Mada, Yogyakarta, Indonesia *romyhanang@ugm.ac.id

Received 2025-02-13, Revised 2025-08-13, Accepted 2025-09-24, Available Online 2025-10-01, Published Regularly October 2025

ABSTRACT

The f(R) gravity theory is a modification of general relativity that yields a Yukawa gravitational potential in the weak-field limit. This potential modifies the Newtonian potential by adding an exponential term that depends on the parameters δ and Λ . In this study, we test the consistency of the Yukawa potential with observational data on the perihelion precession of planets in the solar system. Using observational data from the planets, we estimate the parameters δ and Λ that are consistent with observations. Additionally, we analyze the constraints imposed by the Parametrized Post-Newtonian (PPN) formalism on these parameters. The results indicate that the parameter Λ can be taken within the range [20; 30]AU, with a relatively small value of δ . Observational constraints from the Cassini and MESSENGER missions also provide tight bounds on the PPN parameters γ and β . These findings suggest that the Yukawa potential in f(R) gravity can explain gravitational phenomena on the scale of the solar system without violating existing observational constraints.

Keywords: Yukawa potential; f(R) gravity; Solar system constraints.

INTRODUCTION

The dynamics of celestial bodies within our planetary system offer a unique testing ground for probing gravitational interactions. While Einstein's theory of general relativity (GR) remains the cornerstone of modern gravitational physics [1], its predictions have been scrutinized through phenomena such as the anomalous perihelion advance of Mercury and light deflection measurements. Recent advances in astronomical instrumentation have enabled precision tests of GR in extreme environments, including observations of stellar orbits around the Milky Way's central supermassive black hole. Notably, the pericenter drift and spectral shifts of the S2 star, monitored via the Very Large Telescope [2,3], align with GR's predictions within observational uncertainties.

Despite GR's empirical successes, theoretical challenges persist. The unresolved nature of spacetime singularities [4] and the empirical necessity of dark sector components (dark matter, DM; dark energy, DE) in cosmological frameworks [5–7] motivate explorations of alternative gravity theories. While DM is invoked to explain galactic rotation curves and large-scale structure formation [8–10], and DE accounts for cosmic acceleration [11,12], experimental searches have yet to confirm the existence of DM particles [13,14]. Similarly, the cosmological constant paradigm faces a fundamental theoretical challenge: the predicted vacuum energy density from quantum field theory exceeds observational measurements by 120 orders of magnitude [7,15,16]. These tensions suggest that gravitational physics might require revision at cosmological scales [17,18]

One of the most studied extensions of GR is f(R) gravity, which replaces the Ricci scalar R in the gravitational Lagrangian with a general function f(R). In cosmology, f(R) gravity modifies the Friedmann-Lemaitre equations, enabling self-accelerated expansion without the need for DE $^{[8,19,20]}$ and providing an explanation for inflation without introducing additional scalar fields $^{[4]}$. It also reproduces flat rotation curves in galaxies without invoking DM $^{[9]}$. f(R) gravity introduces a scalar degree of freedom, the scalaron $\psi = df(R)/dR$, which modifies the Schwarzschild metric $^{[21]}$. The gravitational potential in f(R) gravity includes a Yukawa correction term representing a fifth force $^{[21,22]}$.

The precession of the perihelion, which refers to the gradual shift of the closest point of a planet in its orbit around the Sun, is one of the key predictions of general relativity. However, in the context of f(R) gravity, this precession can be modified due to the presence of a Yukawa potential. By comparing theoretical predictions with observational data on the perihelion precession of planets in the solar system, we can estimate the Yukawa potential parameters δ and Λ that are consistent with observations. On the other hand, the formalism known as the Parametrized Post-Newtonian (PPN) formalism provides a framework for testing deviations of alternative gravity theories from Newtonian gravity in the weak-field limit. PPN parameters such as γ and β can be calculated in the context of f(R) gravity and compared with high-precision observational results, such as radio signal time delay measurements from the Cassini mission and observations of Mercury's perihelion precession from the MESSENGER mission.

In this study, we investigate the Yukawa potential generated by f(R) gravity and determine the Yukawa potential parameters by considering two constraints: perihelion precession and the PPN formalism. It is expected that a simpler mechanism can be obtained for determining the Yukawa potential parameters of f(R) gravity, which will ultimately be useful as a local-scale viability test for a given f(R) gravity model.

METHOD

A. Yukawa-like Nonlinear Correction to Gravitational Potential

Yukawa-like potentials represent a class of modified gravitational frameworks that extend beyond the classical Newtonian paradigm by introducing an exponential decay term. These potentials are characterized by deviations from the inverse-square law, which is a cornerstone of Newtonian gravity. Such modifications are particularly relevant in scenarios where traditional gravitational theories fail to account for observed phenomena, such as in the vicinity of compact objects or on cosmological scales. The inclusion of Yukawa-like terms provides a mechanism to address these discrepancies, offering a more nuanced description of gravitational interactions.

Theoretical investigations into Yukawa-like potential have explored their implications across a wide range of scales. Shortrange modifications, typically analyzed in the context of high-energy physics or local gravitational systems, have been discussed in works such as ^[23]. These studies often focus on sub-millimeter scales, where deviations from Newtonian gravity could signal new physics. On the other hand, long-range modifications have been applied to astrophysical systems, including galaxy clusters ^[24,25], the rotation curves of spiral galaxies ^[26], and binary pulsar systems ^[27,28]. These applications aim to explain gravitational anomalies that cannot be fully accounted for by general relativity alone. Additionally, constraints on long-range Yukawa corrections have been explored in works such as ^[29–35], which examine both theoretical predictions and observational limits.

In the context of modified gravity theories, Yukawa-like corrections can be derived from an action principle in the Newtonian limit. The action is given by:

$$S = \int d^4x \sqrt{-g} [f(R) + \mathcal{X} \mathcal{L}_m], \qquad \mathcal{X} = \frac{16\pi G}{c^4}$$
 (1)

where f(R) is a function of the Ricci scalar R, enabling deviations from standard general relativity. The parameter \mathcal{X} , which incorporates the gravitational constant G and the speed of light c, determines the coupling strength between matter and gravity in this modified framework.

The field equations derived from this action are fourth-order differential equations, which are more complex than the second order Einstein field equations. These modified field equations take the form:

$$f'(R)R_{\mu\nu} - \frac{1}{2}f(R)g_{\mu\nu} - f'(R)_{;\mu\nu} + g_{\mu\nu} \Box f'(R) = \frac{\mathcal{X}}{2}T_{\mu\nu}$$
 (2)

where f'(R) denotes the derivative of f(R), and $T_{\mu\nu}$ is the stress-energy tensor. These equations govern the dynamics of the gravitational field, incorporating non-linear contributions from the Ricci scalar R.

To analyze the behavior of these equations in weak-field regimes, the trace of the field equations is often considered:

$$3 \Box f'(R) + f'(R)R - 2f(R) = \frac{x}{2}T$$
 (3)

This trace equation provides insights into the scalar degree of freedom introduced by the modification. The function f(R) can be expanded around R = 0 (corresponding to flat Minkowski spacetime) using a Taylor series:

$$f(R) = \sum_{n=0}^{\infty} \frac{f^{(n)}(0)}{n!} R^n = f_0 + f_1 R + \frac{f_2}{2} R^2 + \dots$$
 (4)

This expansion is particularly useful for studying weak-field gravitational phenomena, as it allows for a systematic approximation of the modified potential.

Under the assumption of spherical symmetry, the metric can be expressed in the form:

$$ds^{2} = \left[1 + \frac{2\Phi(r)}{c^{2}}\right]c^{2}dt^{2} - \left[1 - \frac{2\Psi(r)}{c^{2}}\right]dr^{2} - r^{2}d\Omega^{2}$$
 (5)

where $\Phi(r)$ and $\Psi(r)$ represent the modified gravitational potentials. These potentials are given by:

$$\Phi(r) = -\frac{GM}{(1+\delta)r} \left(1 + \delta e^{-r/\Lambda} \right), \qquad \Psi(r) = \frac{GM}{(1+\delta)r} \left[\left(1 + \frac{r}{\Lambda} \right) \delta e^{-r/\Lambda} - 1 \right]. \tag{6}$$

Here, Λ defines the characteristic length scale of the interaction, while δ quantifies the strength of the modification. These parameters play a crucial role in determining how the gravitational potential deviates from the Newtonian form at different distances.

The choice of the metric ansatz in Eq. (5) is motivated by the physical conditions relevant to solar system tests of gravity. We assume a static, spherically symmetric spacetime, which is a well-justified approximation for the gravitational field of an isolated, non-rotating massive body like the Sun. Furthermore, we work in the weak-field and low-velocity limit, where gravitational potentials are small $(|\Psi(r)|, |\Phi(r)| \ll c^2)$ and time derivatives are negligible. This allows us to treat the metric as a linear perturbation around the Minkowski spacetime, a standard approach in the Parametrized Post-Newtonian (PPN) formalism. In this regime, $\Phi(r)$ and $\Psi(r)$ represent the dominant gravitational potentials that govern planetary orbits and light propagation. In general relativity, spherical symmetry and the vacuum field equations imply $\Phi(r) = \Psi(r)$, leading to the Schwarzschild solution. However, in f(R) gravity, the additional scalar degree of freedom modifies the structure of the field equations, resulting in $\Phi(r) \neq \Psi(r)$. This deviation is a key signature of the theory and gives rise correction term in the Newtonian potential, as shown in Eq. (6). The ansatz (5) thus provides a general framework to capture such deviations while remaining consistent with observational constraints in the solar system.

The correction term to the Newtonian gravitational potential has significant implications for the dynamics of astrophysical systems. For instance, it can affect the orbital precession of test particles, thereby offering a potential observational signature of modified gravity. This type of potential resembles the Yukawa interaction term and is thus commonly referred to as the Yukawa-like potential, or simply the Yukawa gravitational potential. In the weak-field approximation, the modified potential $\Phi(r)$ is given by [36–38]:

$$\Phi(r) = \Phi_Y(r) = -\frac{GM}{(1+\delta)r} \left(1 + \delta e^{-\frac{r}{\Lambda}}\right) \tag{7}$$

Here, Λ is related to the parameters of the f(R) function through $\Lambda^2 = -\frac{f_1}{f_2}$, where f_1 and f_2 are coefficients in the Taylor expansion of f(R). The parameter δ , defined as $\delta = f_1 - 1$, determines the magnitude of the Yukawa correction, which becomes significant in regions where $r \ll \Lambda$.

Recent studies have also explored the implications of Yukawa-like potentials in the context of dark matter and dark energy. For example, the exponential term in the potential can mimic the effects of dark matter on galactic rotation curves, providing an alternative explanation for the observed dynamics without invoking exotic particles [18,37]. Additionally, Yukawa-like modifications have been proposed as a possible mechanism for explaining the accelerated expansion of the universe, offering a geometric alternative to dark energy [29,31]. Therefore, Yukawa-like potentials provide a versatile framework for exploring modifications to gravity, with applications ranging from local gravitational systems to cosmological scales. By incorporating exponential corrections to the Newtonian potential, these models offer a rich phenomenology that can be tested against observational data. Future studies will continue to refine the constraints on the parameters Λ and δ , shedding light on the nature of gravity and its deviations from classical and relativistic predictions.

B. Orbital Precession and Perturbations to Newtonian Gravity

Orbital precession-the gradual rotation of an orbit's major axis-serves as a sensitive probe of gravitational physics. This phenomenon arises from perturbations to the Newtonian potential, which may originate from relativistic effects, extended gravitational theories, or non-inverse-square interactions. In Yukawa-like modified gravity, deviations from the Newtonian potential

introduce additional precession components that can be quantified through perturbative methods.

The angular precession $\Delta \varphi$ per orbital period due to a perturbing potential V(r) is derived from the integral expressions [39,40]:

$$\Delta \varphi^{\text{rad}} = \frac{-2L}{GMe^2} \int_{-1}^{1} \frac{zdz}{\sqrt{1-z^2}} \frac{dV(z)}{dz} = \frac{2}{GMe} \int_{0}^{\pi} \cos \varphi r^2 \frac{dV(r)}{dr} d\varphi \tag{8}$$

where V(z) and V(r) denote the perturbing potential in axial and radial coordinates, respectively. The radial coordinate r relates to z via r = L/(1 + ez), with $L = a(1 - e^2)$ representing the semi-latus rectum, a the semi-major axis, and e the orbital eccentricity.

In General Relativity (GR), the Schwarzschild precession is a hallmark prediction:

$$\Delta \varphi_{\rm GR}^{\rm rad} \approx \frac{6\pi GM}{c^2 a(1-e^2)}$$
 (9)

This result arises purely from spacetime curvature. In contrast, Yukawa gravity modifies the Newtonian potential as $\Phi_Y(r) = -\frac{GM}{(1+\delta)r} \left(1 + \delta e^{-r/\Lambda}\right)$ (see Eq. 7), introducing a perturbing potential:

$$V_Y(r) = \Phi_Y(r) + \frac{GM}{r} = \frac{\delta}{1+\delta} \frac{GM}{r} \left[1 - e^{-r/\Lambda} \right]$$
 (10)

For $r \ll \Lambda$, this potential expands as:

$$V_Y(r) \approx -\frac{\delta GMr}{2(1+\delta)\Lambda^2} \left[1 - \frac{r}{3\Lambda} + \frac{r^2}{12\Lambda^2} - \cdots \right]$$
 (11)

Substituting this into Eq. 8 yields the Yukawa-induced precession:

$$\Delta \varphi_Y^{\rm rad} \approx \frac{\pi \delta \sqrt{1 - e^2}}{1 + \delta} \left(\frac{a^2}{\Lambda^2} - \frac{a^3}{\Lambda^3} + \frac{4 + e^2}{8} \frac{a^4}{\Lambda^4} - \cdots \right) \tag{12}$$

The leading term scales as a^2/Λ^2 , highlighting the sensitivity of precession to the interplay between orbital scale (a) and Yukawa interaction range (Λ). Table I summarizes observed perihelion precession rates for solar system planets. GR predictions align closely with observations, but residuals provide bounds on Yukawa parameters δ and Λ .

The Parametrized Post-Newtonian (PPN) framework quantifies deviations from GR through Eddington parameters γ and β . In isotropic coordinates, the metric expands as ^[1]:

$$ds^{2} \simeq \left[1 - \alpha \frac{r_{g}}{\tilde{r}} + \frac{\beta}{2} \left(\frac{r_{g}}{\tilde{r}}\right)^{2} + \cdots\right] dt^{2} - \left(1 + \gamma \frac{r_{g}}{\tilde{r}} + \cdots\right) (d\tilde{r}^{2} + \tilde{r}^{2} d\Omega^{2}) \tag{13}$$

where $r_g = 2GM/c^2$. In GR, $\gamma = \beta = 1$; deviations signal new physics. For f(R) gravity, the PPN parameters are ^[42]:

$$\gamma - 1 = -\frac{f''(R)^2}{f'(R) + 2f''(R)^2}, \beta - 1 = \frac{1}{4} \left(\frac{f'(R)f''(R)}{2f'(R) + 3f''(R)^2} \right) \frac{d\gamma}{dR}$$
(14)

High-precision tests constrain these parameters: Cassini tracking gives $\gamma - 1 = (2.1 \pm 2.3) \times 10^{-5}$ [43], while Mercury's precession yields $\beta - 1 = (-1.6 \pm 1.8) \times 10^{-5}$ [44].

For f(R) gravity expanded as $f(R) = f_0 + f_1 R + \frac{f_2}{2} R^2 + \cdots$, the Yukawa parameters δ and Λ map to PPN coefficients. Using $f'(R) \approx (\delta + 1) - \frac{(\delta + 1)}{\Lambda^2} R$ and $f''(R) \approx -\frac{(\delta + 1)}{\Lambda^2}$, we derive:

$$\gamma \approx 1 - \frac{\delta + 1}{\Lambda^4 + 2(\delta + 1)} \tag{15}$$

$$\beta - 1 \approx \frac{1}{4} \frac{(\delta + 1)^2}{\Lambda^6 (2\Lambda^2 - 3(\delta + 1)) \left(1 + \frac{2(\delta + 1)}{\Lambda^4}\right)^2}$$
 (16)

These expressions enable direct tests of Yukawa gravity using solar system data, constraining δ and Λ to levels compatible with GR. Yukawa-like modifications to gravity introduce measurable precession effects that depend on the interaction range Λ and coupling strength δ . Current solar system observations tightly constrain these parameters, favoring GR but leaving room for small deviations detectable in future high-precision experiments. The PPN formalism bridges theoretical predictions with empirical tests, providing a robust framework for probing modified gravity across scales.

Table 1: Observed values for various planets, including the semi-major axis (a), orbital period (P), inclination angle (i), eccentricity (e), observed orbital precession ($\dot{\omega}_{obs}$), and the orbital precession predicted by General Relativity ($\dot{\omega}_{GR}$). Adapted from [41].

Planet	a (AU)	P (yrs)	i (degrees)	ϵ	Precession (1)/100yrs)		
					$\dot{\omega}_{obs}$	$\dot{\omega}_{GR}$	
Mercury	0.39	0.24	7.0	0.206	43.1000 ± 0.5000	43.5	
Venus	0.72	0.62	3.4	0.007	8.0000 ± 5.0000	8.62	
Earth	1.00	1.00	0.0	0.017	5.0000 ± 1.0000	3.87	
Mars	1.52	1.88	1.9	0.093	1.3624 ± 0.0005	1.36	
Jupiter	5.20	11.86	1.3	0.048	0.0700 ± 0.0040	0.0628	
Saturn	9.54	29.46	2.5	0.056	0.0140 ± 0.0020	0.0138	

RESULTS AND DISCUSSION

Eq.(14) is a crucial expression for describing the perihelion precession of planets under the influence of the Yukawa potential. This equation demonstrates that the perihelion precession is determined by the orbital parameters of the planet, namely the semi-major axis a and eccentricity e, as well as the Yukawa potential parameters δ and Λ . Since these orbital parameters, including the perihelion precession, are observable physical quantities, they can be directly compared with observational data, such as those presented in Table I. Using Eq. 14 and the orbital data from the table, we obtain plots of the parameter δ as a function of Λ for each planet, as shown in Figures 1, 2, and 3. In these figures, the curves for δ_{\min} and δ_{\max} correspond to the minimum and maximum values of the observed perihelion precession $\dot{\omega}_{\rm obs}$, as listed in Table 1. Additionally, reference values of $\delta=1$ and $\delta=0.1$ are plotted for comparison, which will be discussed further in the following sections.

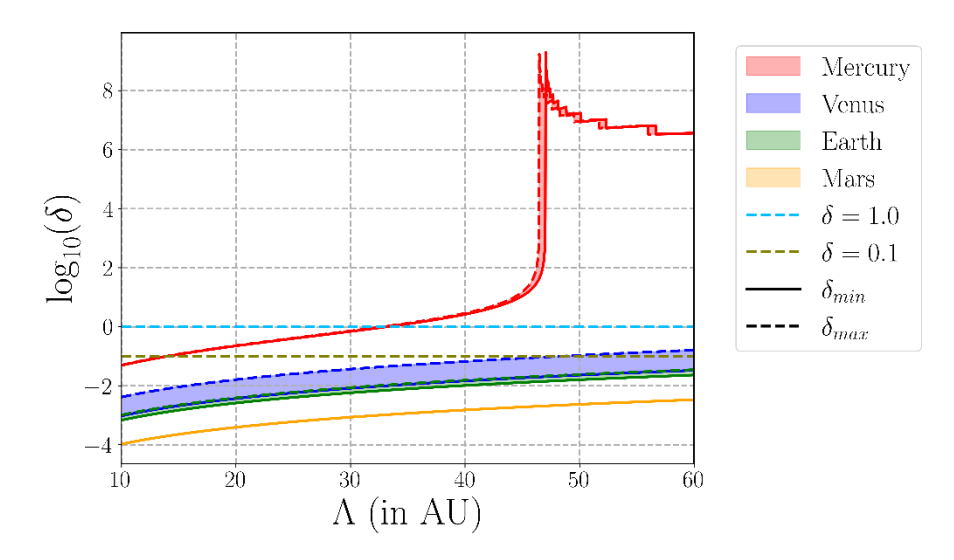


Figure 1: Variation of δ as a function of Λ for Mercury to Mars.

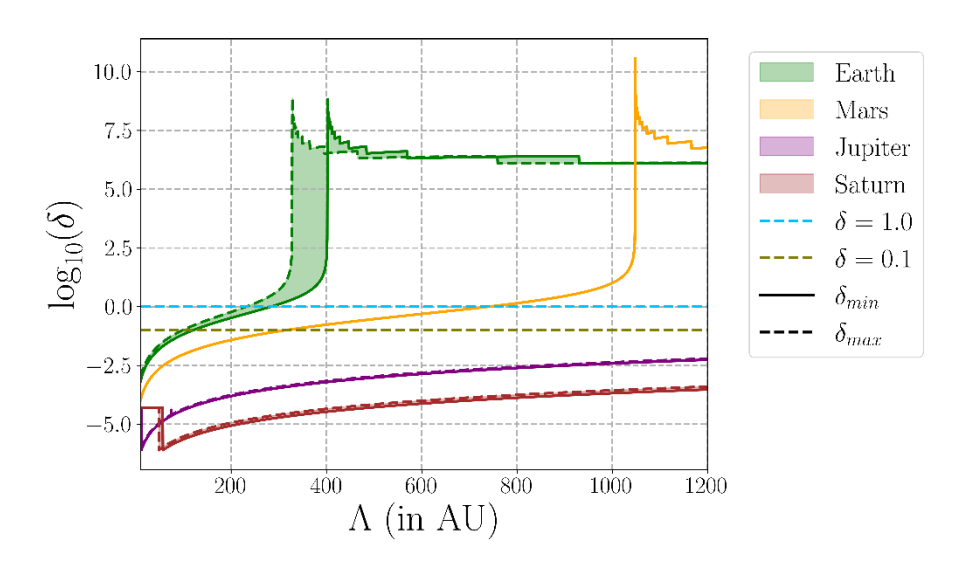


Figure 2: Variation of δ as a function of Λ for Earth to Saturn.

To facilitate data presentation and analysis, the plots for all planets are displayed separately, allowing for a detailed examination of the behavior of δ across different ranges of Λ . From Figures 1, 2, and 3, it is evident that δ tends to be small ($\delta \ll 1$) for small values of Λ , gradually increases to order unity, and then rises sharply beyond a certain threshold value of Λ . If we denote Λ_p as the value of Λ at which δ begins to increase rapidly, we observe a trend where Λ_p is proportional to the planet's distance from the Sun, or equivalently, to the semi-major axis α . Another notable feature is that, after this rapid increase, δ asymptotically approaches a large value ($\simeq 10^7$) at large Λ , with the exact value depending on the specific planet. Furthermore, δ_{\min} and δ_{\max} tend to converge in the region where $\delta < 1$.

The Yukawa gravitational potential in Eq. 12 indicates that, in the weak-field regime where the Yukawa potential can be treated as a perturbation to the Newtonian potential, the parameter δ must be sufficiently small ($\delta \ll 1$), and Λ must be much larger than the orbital scale ($r \ll \Lambda$). However, as shown in Figures 1, 2, and 3, very large values of Λ tend to drive δ toward an asymptotically large value ($\simeq 10^7$). This suggests that if the Yukawa potential is assumed to

be effective within the solar system, the parameters Λ and δ must be carefully chosen to ensure consistency across all planets.

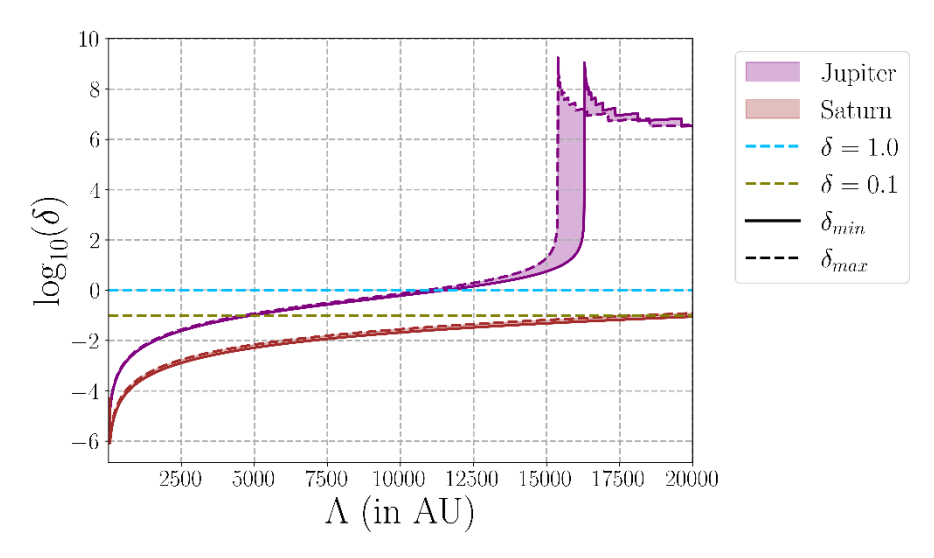


Figure 3. Variation of δ as a function of Λ for Jupiter and Saturn.

If we impose the condition $\delta \ll 1$ on Eq. 12, we find that the values of Λ for each planet generally satisfy the requirement $r \ll \Lambda$. For example, for Jupiter, which has a semi-major axis $a \simeq 9.54 \mathrm{AU}$ (see Figure 3), δ remains very small ($\delta < 0.1$) for $\Lambda < 10^4 \mathrm{AU}$. In contrast, for Mercury (see Figure 1), the relevant values of δ correspond to $\Lambda < 15 \mathrm{AU}$. Therefore, if we apply a strict upper limit of $\delta \leq 0.1$ for all planets, the most stringent constraint on Λ arises from Mercury, yielding $\Lambda \leq 15 \mathrm{AU}$, as shown in Figure 1. For comparison, the values of δ_{\min} and δ_{\max} for $\Lambda = 20 \mathrm{AU}$, 30 AU, 35 AU, and 40 AU are also presented in Table 2. The table also includes the average values $\delta \pm \Delta \bar{\delta}$ for all planets at each Λ , as well as estimates of the PPN parameters $\gamma - 1$ and $\beta - 1$ derived from Eqs. 15 and 16.

Table 2 shows that the average value of δ for the solar system planets remains small up to $\Lambda =$ 40 AU. However, since $\bar{\delta} + \Delta \bar{\delta} \simeq 1.52$, which violates the assumption $\delta \ll 1$, data for $\Lambda \geq$ 40AU can reasonably be disregarded. To further refine the selection of Yukawa parameters, we consider the constraints on the PPN parameters ν and β , which are tightly constrained by observations from the Cassini and MESSENGER missions to the ranges $\gamma - 1 =$ $[-0.2; 4.4] \times 10^{-5}$ and $\beta - 1 = [-3.4; 0.2] \times 10^{-5}$, respectively. Applying these constraints, we find that only $\Lambda = 15$ AU satisfies the PPN limits. In summary, the numerical calculations in this study suggest that the Yukawa parameter Λ can be chosen within the range [20, 30] AU, with corresponding average values of $\bar{\delta} \pm \Delta \bar{\delta}$. Specifically, we obtain $\bar{\delta} \pm \Delta \bar{\delta} = 0.0401216 \pm 0.040120 \pm 0.040120 \pm 0.040120 \pm 0.040120 \pm 0.040120 \pm 0.040120 \pm$ 0.0874637 for $\Lambda = 20$ AU, $\bar{\delta} \pm \Delta \bar{\delta} = 0.1227306 \pm 0.2725966$ for $\Lambda = 30$ AU, and $\bar{\delta} \pm 0.0874637$ $\Delta \bar{\delta} = 0.2209792 + 0.4969559$ for $\Lambda = 35$ AU. These results are consistent with previous studies, such as [45-49], which investigated the effects of the Yukawa potential on the S-star population near the galactic center and found $\Lambda > 5000 \mathrm{AU}$ with $\delta \approx 10^{-3}$. However, our results align more closely with solar system studies, such as [50,51], which reported $\Lambda \approx$ 0.182AU and $\delta \approx 2 \times 10^{-10}$ for Earth and Mercury. This highlights the strong dependence of the Yukawa potential's influence on the scale of the gravitational source, with the Sun's influence being significantly smaller than that of galactic-scale sources [52–54].

Planet	$\Lambda = 15 \text{AU}$		$\Lambda=20\mathrm{AU}$		$\Lambda = 30 \text{AU}$		$\Lambda = 35 \text{AU}$		$\Lambda=40\mathrm{AU}$	
	δ_{min}	$\delta_{\sf max}$								
Mercury	0.115518	0.118552	0.223865	0.230331	0.691811	0.719739	1.250011	1.318028	2.631403	2.870483
Venus	0.002095	0.009144	0.003686	0.016174	0.008232	0.036682	0.011200	0.050416	0.014640	0.066698
Earth	0.001487	0.002232	0.002602	0.003909	0.005777	0.008691	0.007843	0.011810	0.010231	0.015426
Mars	0.000226	0.000226	0.000392	0.000392	0.000861	0.000862	0.001164	0.001165	0.001512	0.001514
Jupiter	0.000001	0.000001	0.000002	0.000002	0.000004	0.000004	0.000005	0.000006	0.000006	0.000007
Saturn	0.000050	0.000050	0.000050	0.000050	0.000050	0.000050	0.000050	0.000050	0.000050	0.000050
$\bar{\delta} \pm \Delta \bar{\delta}$	0.020798±0.045028		0.040121± 0.087463		0.122730± 0.272596		0.220979± 0.496955		0.467668± 1.067895	
$\gamma - 1$	[-1.93; -2.09]		[-6.11; -6.95]		[-1.06; -1.70]		[-0.51; -1.12]		[-3.03; -8.34]	
	$\times 10^{-5}$		$\times 10^{-6}$		$\times 10^{-6}$		$\times 10^{-6}$		$\times 10^{-7}$	
R - 1	$[4.90 \cdot 4.91] \times 10^{-11}$		$[4.90 \cdot 4.90] \times 10^{-12}$		$[1.90 \cdot 1.90] \times 10^{-13}$		$[5.55 \cdot 5.57] \times 10^{-14}$		$[1.90 \cdot 1.90] \times 10^{-14}$	

Table 2: Values of δ_{min} and δ_{max} for various $\Lambda(AU)$ and its average values $\bar{\delta} \pm \Delta \bar{\delta}$. We also provide the predicted PPN parameters $\gamma - 1$ and $\beta - 1$ based on formula in Eq. 15 and Eq. 16

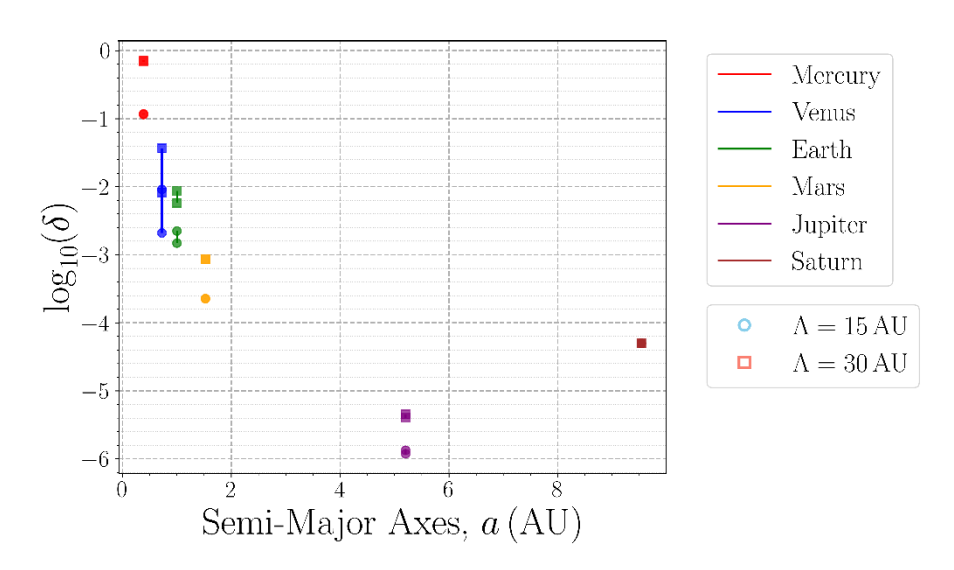


Figure 4. Variation of δ as a function of Semi-major axes α for all planets.

CONCLUSION

The f(R) theory of gravity is a modification of general relativity that extends the gravitational action. In the weak-field limit, f(R) gravity gives rise to a Yukawa gravitational potential $V_Y(r) = \frac{\delta}{1+\delta} \frac{GM}{r} \left[1-e^{-r/\Lambda}\right]$, which deviates slightly from the Newtonian potential. The Yukawa parameters must satisfy $\delta \ll 1$ and $\Lambda \gg r$ to remain consistent with Newtonian gravity in the weak-field regime. To determine the viable ranges for δ and Λ , we employed solar system tests, such as perihelion precession and PPN constraints, which measure deviations from Newtonian gravity.

Perihelion precession, the gradual shift in a planet's closest approach to the Sun, is a small but measurable effect. For example, Mercury's precession is approximately 43.1'' per century. This phenomenon does not occur in Newtonian gravity but is predicted by more complex theories, such as general relativity and f(R) gravity.

In this study, observational data on perihelion precession were used to determine the minimum and maximum values of δ using Eq. 14. The permissible range of Λ was inferred by analyzing the δ plots for all planets. Figures 1, 2, and 3 demonstrate that the tightest constraint on Λ arises from Mercury's data. By calculating the average values $\bar{\delta} \pm \Delta \bar{\delta}$ for each Λ , we applied PPN constraints from Eqs. 15 and 16.

Our numerical results indicate that the Yukawa parameter Λ can be chosen within the range [20;30] AU, with corresponding average values of $\bar{\delta} \pm \Delta \bar{\delta}$. For instance, we obtain $\bar{\delta} \pm \Delta \bar{\delta} = 0.0401216 \pm 0.0874637$ for $\Lambda = 20$ AU, $\bar{\delta} \pm \Delta \bar{\delta} = 0.1227306 \pm 0.2725966$ for $\Lambda = 30$ AU, and $\bar{\delta} \pm \Delta \bar{\delta} = 0.2209792 \pm 0.4969559$ for $\Lambda = 35$ AU. These findings are consistent with previous studies, underscoring the importance of the gravitational source's scale in determining the influence of the Yukawa potential.

It is important to note, however, that this analysis is based on several simplifying assumptions. First, the derivation of the Yukawa potential relies on the linearized approximation of f(R) gravity in the weak-field limit, which may not capture full nonlinear effects present in more general models. Second, the model assumes a static, spherically symmetric spacetime and neglects higher-order perturbations such as the solar quadrupole moment (J_2) and planetary interactions, which could affect the precision of perihelion precession residuals. Third, the Yukawa parameters δ and Λ are treated as universal constants, whereas in realistic f(R) models with screening mechanisms, such as the chameleon mechanism, these parameters may depend on the local matter density, leading to suppressed deviations in high-density regions like the solar system. Therefore, while our results are consistent with current observational constraints, they should be interpreted within the context of the adopted perturbative framework and may benefit from future analyses incorporating high-precision ephemeris models and environmental dependence.

REFERENCES

- Will, C. M. (2014). The confrontation between general relativity and experiment. *Living Reviews in Relativity*, 17(1), 1–117.
- GRAVITY Collaboration, Abuter R., Amorim A., Bauböck M., Berger J. P., Bonnet H., Brandner W., Cardoso V., Clénet Y., de Zeeuw P. T., Dexter J., Eckart A., Eisenhauer F., Förster Schreiber N. M., Garcia P., Gao F., Gendron E., Genzel R., Gillessen S., ... Zins G. (2020). Detection of the Schwarzschild precession in the orbit of the star S2 near the Galactic centre massive black hole. *Astron. Astrophys.*, 636, L5. https://doi.org/10.1051/0004-6361/202037813
- GRAVITY Collaboration, Abuter R., Amorim A., Anugu N., Bauböck M., Benisty M., Berger J. P., Blind N., Bonnet H., Brandner W., Buron A., Collin C., Chapron F., Clénet Y., dCoudé u Foresto V., de Zeeuw P. T., Deen C., Delplancke-Ströbele F., Dembet R., ... Zins G. (2018). Detection of the gravitational redshift in the orbit of the star S2 near the Galactic centre massive black hole . *Astron. Astrophys.*, 615, L15. https://doi.org/10.1051/0004-6361/201833718
- Starobinsky, A. A. (1980). A new type of isotropic cosmological models without singularity. *Phys. Lett. B*, *91*(1), 99–102. https://doi.org/https://doi.org/10.1016/0370-2693(80)90670-X
- Blumenthal, G. R., Faber, S. M., Primack, J. R., & Rees, M. J. (1984). Formation of Galaxies and Large Scale Structure with Cold Dark Matter. *Nature*, 311, 517–525. https://doi.org/10.1038/311517a0

- Peebles, P. ~J. ~E. (1982). Large-scale background temperature and mass fluctuations due to scale-invariant primeval perturbations. *Astrophys. J. Lett.*, 263, L1–L5. https://doi.org/10.1086/183911
- Peebles, P. J. E., & Ratra, B. (2003). The cosmological constant and dark energy. *Rev. Mod. Phys.*, 75(2), 559–606. https://doi.org/10.1103/RevModPhys.75.559
- 8 Capozziello, S. (2002). CURVATURE QUINTESSENCE. *Int. J. Mod. Phys. D*, *11*(04), 483–491. https://doi.org/10.1142/S0218271802002025
- 9 Capozziello, S., Cardone, V. F., & Troisi, A. (2007). Low surface brightness galaxy rotation curves in the low energy limit of Rn gravity: no need for dark matter? *Mon. Not. Roy. Astron. Soc.*, 375(4), 1423–1440. https://doi.org/10.1111/j.1365-2966.2007.11401.x
- 10 Starobinsky, A. A. (2007). Disappearing cosmological constant in f(R) gravity. *JETP Lett.*, 86, 157–163. https://doi.org/10.1134/S0021364007150027
- Perlmutter, S., Aldering, G., Goldhaber, G., Knop, R. A., Nugent, P., Castro, P. G., Deustua, S., Fabbro, S., Goobar, A., Groom, D. E., Hook, I. M., Kim, A. G., Kim, M. Y., Lee, J. C., Nunes, N. J., Pain, R., Pennypacker, C. R., Quimby, R., Lidman, C., ... Project, T. S. C. (1999). Measurements of Ω and Λ from 42 High-Redshift Supernovae. *Astrophys. J.*, *517*(2), 565. https://doi.org/10.1086/307221
- Riess, A. G., Filippenko, A. V, Challis, P., Clocchiatti, A., Diercks, A., Garnavich, P. M., Gilliland, R. L., Hogan, C. J., Jha, S., Kirshner, R. P., Leibundgut, B., Phillips, M. M., Reiss, D., Schmidt, B. P., Schommer, R. A., Smith, R. C., Spyromilio, J., Stubbs, C., Suntzeff, N. B., & Tonry, J. (1998). Observational Evidence from Supernovae for an Accelerating Universe and a Cosmological Constant. *Astron. J.*, *116*(3), 1009. https://doi.org/10.1086/300499
- Abercrombie, D., & others. (2020). Dark Matter benchmark models for early LHC Run-2 Searches: Report of the ATLAS/CMS Dark Matter Forum. *Phys. Dark Univ.*, 27, 100371. https://doi.org/10.1016/j.dark.2019.100371
- PICO Collaboration, Amole, C., Ardid, M., Arnquist, I. J., Asner, D. M., Baxter, D., Behnke, E., Bhattacharjee, P., Borsodi, H., Bou-Cabo, M., Brice, S. J., Broemmelsiek, D., Clark, K., Collar, J. I., Cooper, P. S., Crisler, M., Dahl, C. E., Das, M., Debris, F., ... Zhang, J. (2016). Improved dark matter search results from PICO-2L Run 2. *Phys. Rev. D*, 93(6), 61101. https://doi.org/10.1103/PhysRevD.93.061101
- 15 Carroll, S. M. (2001). The Cosmological constant. *Liv. Rev. Relativ.*, *4*, 1. https://doi.org/10.12942/lrr-2001-1
- Weinberg, S. (1989). The cosmological constant problem. *Rev. Mod. Phys.*, 61(1), 1–23. https://doi.org/10.1103/RevModPhys.61.1
- Odintsov, S. D., Oikonomou, V. K., & Sharov, G. S. (2023). Early dark energy with power-law F(R) gravity. *Phys. Lett. B*, 843, 137988. https://doi.org/https://doi.org/10.1016/j.physletb.2023.137988
- Stabile, A., & Capozziello, S. (2013). Galaxy rotation curves in f(R,φ) gravity. *Phys. Rev. D*, 87(6), 64002. https://doi.org/10.1103/PhysRevD.87.064002
- Carroll, S. M., Duvvuri, V., Trodden, M., & Turner, M. S. (2004). Is cosmic speed-up due to new gravitational physics? *Phys. Rev. D*, 70(4), 43528. https://doi.org/10.1103/PhysRevD.70.043528
- Nojiri, S., & Odintsov, S. D. (2003). Quantum de Sitter cosmology and phantom matter. *Phys. Lett. B*, 562(3), 147–152. https://doi.org/https://doi.org/10.1016/S0370-2693(03)00594-X
- Kalita, S. (2018). Gravitational Theories near the Galactic Center. *Astrophys. J.*, 855(1), 70. https://doi.org/10.3847/1538-4357/aaadbb
- Hees, A., Do, T., Ghez, A. M., Martinez, G. D., Naoz, S., Becklin, E. E., Boehle, A., Chappell, S., Chu, D., Dehghanfar, A., Kosmo, K., Lu, J. R., Matthews, K., Morris, M. R., Sakai, S.,

- Schödel, R., & Witzel, G. (2017). Testing General Relativity with Stellar Orbits around the Supermassive Black Hole in Our Galactic Center. *Phys. Rev. Lett.*, 118(21), 211101. https://doi.org/10.1103/PhysRevLett.118.211101
- Adelberger, E. G., Gundlach, J. H., Heckel, B. R., Hoedl, S., & Schlamminger, S. (2009). Torsion balance experiments: A low-energy frontier of particle physics. *Progress in Particle and Nuclear Physics*, 62(1), 102–134. https://doi.org/https://doi.org/10.1016/j.ppnp.2008.08.002
- Capozziello, S., De Filippis, E., & Salzano, V. (2009). Modelling clusters of galaxies by f (R) gravity. *Monthly Notices of the Royal Astronomical Society*, 394(2), 947–959.
- Capozziello, S., Stabile, A., & Troisi, A. (2007). Newtonian limit of f (R) gravity. *Physical Review D—Particles, Fields, Gravitation, and Cosmology*, 76(10), 104019.
- Cardone, V. F., & Capozziello, S. (2011). Systematic biases on galaxy haloes parameters from Yukawa-like gravitational potentials. *Monthly Notices of the Royal Astronomical Society*, 414(2), 1301–1313. https://doi.org/10.1111/j.1365-2966.2011.18465.x
- Dong, Y., Shao, L., Hu, Z., Miao, X., & Wang, Z. (2022). Prospects for constraining the Yukawa gravity with pulsars around Sagittarius A. *Journal of Cosmology and Astroparticle Physics*, 2022(11), 51.
- Miao, X., Shao, L., & Ma, B.-Q. (2019). Bounding the mass of graviton in a dynamic regime with binary pulsars. *Physical Review D*, 99(12), 123015.
- Amendola, L., & Quercellini, C. (2004). Skewness as a test of the equivalence principle. *Physical Review Letters*, 92(18), 181102.
- Moffat, J. W. (2006). Scalar–tensor–vector gravity theory. *Journal of Cosmology and Astroparticle Physics*, 2006(03), 4.
- Moffat, J. W. (2005). Gravitational theory, galaxy rotation curves and cosmology without dark matter. *Journal of Cosmology and Astroparticle Physics*, 2005(05), 3.
- Reynaud, S., & Jaekel, M.-T. (2005). Testing the Newton law at long distances. *International Journal of Modern Physics A*, 20(11), 2294–2303.
- Sealfon, C., Verde, L., & Jimenez, R. (2005). Limits on deviations from the inverse-square law on megaparsec scales. *Physical Review D—Particles, Fields, Gravitation, and Cosmology*, 71(8), 83004.
- Sereno, M., & Jetzer, P. (2006). Dark matter versus modifications of the gravitational inversesquare law: results from planetary motion in the Solar system. *Monthly Notices of the Royal Astronomical Society*, *371*(2), 626–632.
- White, M., & Kochanek, C. S. (2001). Constraints on the long-range properties of gravity from weak gravitational lensing. *The Astrophysical Journal*, *560*(2), 539.
- Borka, D., Jovanović, V. B., & Jovanović, P. (2023). Bounds on graviton mass and constraining Yukawa-like gravitational potential from planetary motion in the Solar System. *Filomat*, 37(25), 8591–8601. https://doi.org/10.2298/FIL2325591B
- Capozziello, S., Borka, D., Jovanović, P., & Jovanović, V. B. (2014). Constraining extended gravity models by S2 star orbits around the Galactic Centre. *Physical Review D*, 90(4), 44052.
- Yukawa, H. (1935). On the Interaction of Elementary Particles I. *Proc. Phys. Math. Soc. Jap.*, 17, 48–57. https://doi.org/10.1143/PTPS.1.1
- Adkins, G. S., & McDonnell, J. (2007). Orbital precession due to central-force perturbations. *Physical Review D—Particles, Fields, Gravitation, and Cosmology*, 75(8), 82001.
- Chashchina, O. I., & Silagadze, Z. K. (2008). Remark on orbital precession due to central-force perturbations. *Physical Review D—Particles, Fields, Gravitation, and Cosmology*, 77(10), 107502.

- Nyambuya, G. G. (2010). Azimuthally symmetric theory of gravitation—I. On the perihelion precession of planetary orbits. *Monthly Notices of the Royal Astronomical Society*, 403(3), 1381–1391.
- 42 Capozziello, S., & Troisi, A. (2005). Parametrized post-Newtonian limit of fourth order gravity inspired by scalar-tensor gravity. *Physical Review D—Particles, Fields, Gravitation, and Cosmology*, 72(4), 44022.
- 43 Bertotti, B., Iess, L., & Tortora, P. (2003). A test of general relativity using radio links with the Cassini spacecraft. *Nature*, *425*(6956), 374–376.
- Genova, A., Mazarico, E., Goossens, S., Lemoine, F. G., Neumann, G. A., Smith, D. E., & Zuber, M. T. (2018). Solar system expansion and strong equivalence principle as seen by the NASA MESSENGER mission. *Nature Communications*, 9(1), 289.
- D'Addio, A. (2021). S-star dynamics through a Yukawa–like gravitational potential. *Physics of the Dark Universe*, *33*, 100871.
- Kalita, S. (2020). The Galactic Center Black Hole, Sgr A*, as a Probe of New Gravitational Physics with the Scalaron Fifth Force. *Astrophys. J.*, 893(1), 31. https://doi.org/10.3847/1538-4357/ab7af7
- Kalita, S. (2021). Scalaron Gravity near Sagittarius A*: Investigation of Spin of the Black Hole and Observing Requirements. *Astrophys. J.*, 909(2), 189. https://doi.org/10.3847/1538-4357/abded5
- 48 Lalremruati, P. C., & Kalita, S. (2022). Is It Possible to See the Breaking Point of General Relativity near the Galactic Center Black Hole? Consideration of Scalaron and Higher-dimensional Gravity. *Astrophys. J.*, 925(2), 126. https://doi.org/10.3847/1538-4357/ac3af0
- 49 Paul, D., Kalita, S., & Talukdar, A. (2023). Unscreening of f(R) gravity near the galactic center black hole: Testability through pericenter shift below S0-2's orbit. *Int. J. Mod. Phys. D*, *32*(04), 2350021. https://doi.org/10.1142/S0218271823500219
- 50 Iorio, L. (2007). Constraints on the range λ of Yukawa-like modifications to the Newtonian inverse-square law of gravitation from Solar System planetary motions. *Journal of High Energy Physics*, 2007(10), 41.
- Iorio, L. (2009). The recently determined anomalous perihelion precession of Saturn. *The Astronomical Journal*, 137(3), 3615.
- Cardone, V. F., Angus, G., Diaferio, A., Tortora, C., & Molinaro, R. (2011). The modified Newtonian dynamics fundamental plane. *Monthly Notices of the Royal Astronomical Society*, 412(4), 2617–2630.
- D'Agostino, R., Jusufi, K., & Capozziello, S. (2024). Testing Yukawa cosmology at the Milky Way and M31 galactic scales. *The European Physical Journal C*, 84(4), 1–17.
- Jusufi, K., Leon, G., & Millano, A. D. (2023). Dark Universe phenomenology from Yukawa potential? *Physics of the Dark Universe*, 42, 101318.